International Conference
Nuclear Energy for New Europe 2007
Portorož /Slovenia /September 10-13
port2007@ijs.si
www.nss.si/port2007
+386 1 588 5247, fax +386 1 588 5376
PORT2007, Nuclear Society of Slovenia, Jamova 39, SI-1000 Ljubljana, Slovenia

Heat and Mass Transfer in the Stratified Flow with ECCS Injection

Luka Štrubelj, Iztok Tiselj
"Jožef Stefan" Institute
Jamova 39, SI-1000 Ljubljana, Slovenia
luka.strubelj@ijs.si, iztok.tiselj@ijs.si

ABSTRACT

One of the most important problems in the light-water nuclear thermal-hydraulics is behaviour of the cold emergency core cooling water injected from the top or from the bottom into the horizontal section of the cold leg near the reactor vessel during the loss of coolant accident. The stratified flows appear where cold water is injected in partially or fully uncovered horizontal cold leg. The hot steam condenses on cold water surface what is also called direct contact condensation. Direct contact condensation and condensation induced water-hammer in a horizontal pipe were experimentally investigated at PMK-2 test facility of the Hungarian Atomic Energy Research Institute KFKI. The cold water is injected through small pipe into lower horizontal part of the section, and then water fills the vertical pipeline and floods the horizontal test section of the pipeline of the PMK-2 integral test facility. As liquid water floods the horizontal part of the pipeline, the counter current horizontally stratified flow is being observed. During the flooding of the pipeline, the steam-liquid interface area increases and therefore the steam condensation rate and the steam velocity also increase and can lead to bubble entrapment. Water level at one cross-section and four local void fraction and temperature at the top of horizontal test pipeline was measured and compared with simulation. Condensed steam increases the water temperature that is why the local temperature measurements are the most important information, from which condensation rate can be estimated, since mass of condensed steam was not measured. Numerical simulation of the experiment with thermal phase change is presented. Surface renewal concept with small eddies is used for calculation of condensation heat transfer coefficient. Two simulations were performed: simulation of whole experimental domain (lower horizontal, vertical and test horizontal pipeline) and simplified simulation of only upper horizontal test section. In both numerical simulations the condensation rate is significantly increased during bubble entrapment and its condensation. The local temperatures in experiment are compared with simulation.

1 INTRODUCTION

Only a limited analytical approach to the problem of DCC in horizontal stratified flow is possible, therefore experiments are necessary. There were a lot of experiments done to analyze and understand the DCC phenomena [1-5]. Several integral condensation correlations were developed with Nusselt number as function of liquid Prandtl and Reynolds number and gas Reynolds number. Two frequently used condensation correlations for heat and mass transfer during the DCC in stratified flow were derived from experimental results by Lim et al. [1] and Kim, Lee and Bankoff [2]. Integral condensation correlations are based on bulk flow properties and are valid only in a specified range of parameters and geometry (usually

pipe or channel). More precise modelling can be done with Computational Fluid Dynamics (CFD) codes, where local condensation correlations with one of techniques for simulation of stratified flow are used. Local condensation correlations are based on local flow properties, usually turbulent quantities, and can be used for all geometries.

Several attempts to model DCC can be found in the literature. Simulations of stratified flow with a 2D two-fluid model are performed by Yao et al. [3], who made simulations of stratified flow with and without the condensation. Experiments and models of DCC in a rectangular duct and rectangular tank were described by Lorencez et al. [4] and Mikielewicz et al. [5]. Especially Lorencez et al. [4] with their sophisticated experiment made a detailed measurement of the turbulence near the free surface and clarified the impact of the turbulence on the interfacial heat and mass transfer coefficients. Hughes and Duffey [6] introduced a "surface renewal theory" for DCC in turbulent separated flow, which points to an important role of the turbulence in the liquid layer. 2D CFD simulations of ECC injection of subcooled water into horizontally stratified hot leg flow (experimental device COSI) were performed by Coste [7] using two-fluid model with interfacial heat and mass transfer model based on surface renewal concept [6]. Experiment on COSI experimental device was also simulated by Boucker et al. [8] with CFD code Neptune_CFD [9] who also used surface renewal concept [6].

Our objective is to validate the condensation model, from the water heat up in experiments, which is mainly due to condensation. During ECCS injection in partially or fully uncovered cold leg, the pressurized thermal shock occurs, where the cold water temperature is important parameter and should be predicted with good accuracy.

2 EXPERIMENTS

A set of experiments with improved steam volume fraction measurement was run at Hungarian KFKI experimental device PMK-2 (Prasser et al. [10] and [11]) within the WAHALoads project of the 5th EU research program. Attempts to describe the KFKI experiment with the 1D two-fluid model of the WAHA code (Tiselj et al. [12]) pointed to large uncertainties of the simulations related to the model of stratified-to-slug flow transition and correlations for interfacial heat, mass and momentum transfer. Gale [13], [14] smoothen the transition from stratified to disperse flow and condensation mass transfer during the transition in WAHA Code, and improved agreement of pressure peaks in simulation with pressure peaks measured in KFKI experiment.

Test section of the water hammer facility consists of a 3,2 m long horizontal pipe with inner diameter 73 mm. Steam generator supplies steam for the test section. Pipeline section connected to the condenser is isolated in the water hammer experiment. The supply of cold water is obtained with a 75 litre water tank pressurized with nitrogen. Water is injected thru pipe with inner diameter of 24 mm, connected to lower horizontal pipe, by opening the valve in the injection line.

All together, 35 water hammer experiments at the PMK-2 device were performed, at initial steam pressures between 10 and 40 bar and at cold water temperatures between 17 and 140 °C. Cold water mass flow rates were between 0.7 and 1.7 kg/s. Before the start of each experiment the whole construction was heated with steam for a few hours. Steam pressure in the pipe and water tank flow rate can be considered as constant during the transient. Experiments performed at PMK-2 are described in the reports by Prasser et al. [10], [11]. The most important results for the present paper are actually local void and temperature measurements, and not the water hammer pressure peaks. From the local void measurements and wire mesh sensor entrapment of the steam bubble can be seen. The reason for the bubble entrapment can not be explained from the experiment data. Two reasons are possible:

entrapment is due to interface instability, believed to be the Kelvin-Helmholtz instability, because relative velocity is high enough that free surface gets in touch with the upper pipe wall. The other possibility is entrapment of the steam bubble due to the wave reflection from the end of the pipe. Results of numerical simulations showed that bubble entrapment is due to surface instability. It is important to stress the rather large uncertainty of the experiments - especially the maximum pressure peaks recorded: two experiments performed at very similar initial conditions can give very different pressure peaks with a difference of factor ~2 not uncommon.

3 NUMERICAL SIMULATIONS

In present work only the simulation of experimental case without water hammer was performed. The pipe domain was discretized with a structured grid. We used from 400 up to 24,500 hexa elements. The meshes on fig. 2-4 are named Hn, where n stands for number of elements in pipe height. The geometry and boundary conditions can be seen on fig 1. Initially pipe is fully filled with steam at saturation at 30 bar. The injected water temperature is 97°C (subcooling of 137°C). The steam is supplied at saturation conditions (30 bar).

Numerical simulation was performed with Neptune_CFD code [9]. More about models and numerical methods can be found in Neptune_CFD documentation [9]. Simulations with Neptune_CFD are performed with real gas properties (CATHARE code steam tables – pressured and temperature dependent properties). One continuity, momentum and energy equations were solved with the k-ε turbulent models for each phase. The conservation of mass in our simulations is 0.15 %.

The interphase mass transfer per unit volume due to condensation is calculated as $\Gamma = \dot{m}A$, where interphase area density is calculated as $A = |\nabla \alpha|$. Interphase mass flow rate per unit of interfacial area is calculated from liquid heat transfer coefficient HTC_L, difference between saturation enthalpy of steam $h_{S,sat}$ and liquid enthalpy h_L, and difference between saturation temperature $T_{sat} = T_{sat}(p)$ and liquid temperature T_L

$$\dot{m} = \frac{HTC_L(T_{sat} - T_L)}{h_{S,sat} - h_L} \tag{1}$$

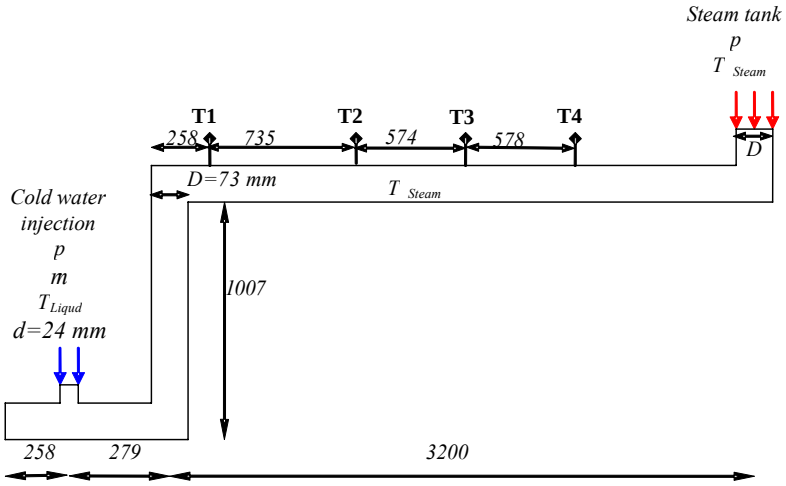

Figure 1: Numerical domain with boundary conditions and local measurements of temperature (p=30 bar, T_{Liquid}=97°C, T_{Steam}=234 °C, $\dot{m}$=1 kg/s).

The heat transfer coefficient was calculated using surface renewal theory introduced by Hughes and Duffey [6]:

$$HTC_L = \frac{2}{\sqrt{\pi}} \frac{\rho_L c_{p,L}}{\nu_L} (a_L)^{1/2} u_t = \frac{2}{\sqrt{\pi}} \frac{\lambda_L}{\nu_L} \mathrm{Pr}^{1/2} u_t \quad (2)$$

$$u_t = C_\mu^{1/4} k_L^{1/2}; \; C_\mu = 0.09 \quad (3)$$

In equations above u_t is velocity scale, Pr Prandtl number, ρ_L liquid density, $c_{p,L}$ liquid specific heat capacity at constant pressure, λ_L thermal conduction, ν_L liquid viscosity and k_L liquid turbulence kinetic energy modelled with turbulence model. The maximum heat transfer coefficient observed in simulations is 2,000,000 W/m^{2}K, average is about 10-times smaller. The local interfacial mass transfer rate is up to 2000 kg/m^3/s, average is about 10-times smaller.

3.1 Simplified numerical simulation

First we performed numerical simulation of only upper horizontal part where measurements are available.

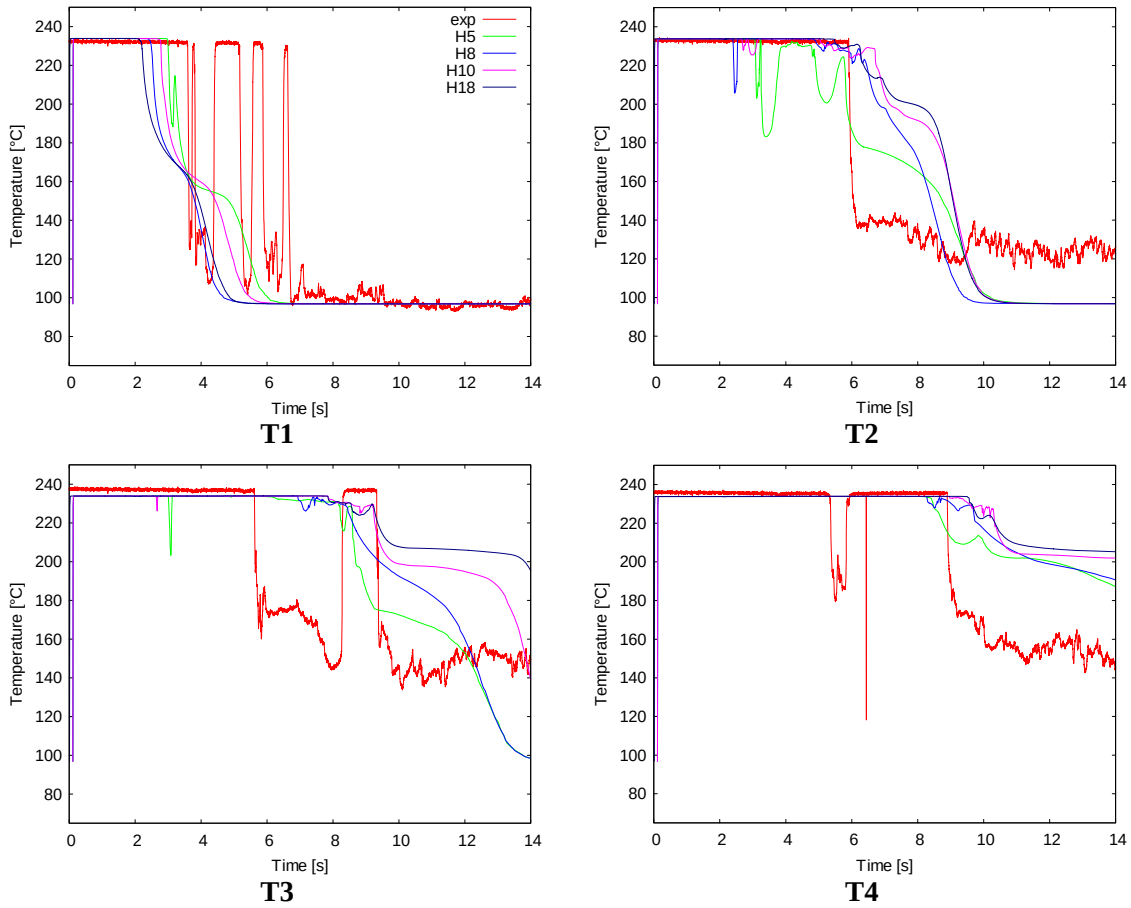

Figure 2**:** Local temperatures in simplified numerical simulations on different meshes and experiment at 4 measurement points.

The local temperature development on 4 measuring points in the experiment (red line) and in the numerical simulations on four different meshes is presented on fig. 2. On the

measurement point T1, which is the nearest to the transition from vertical to upper horizontal part, several bubble entrapments appear in the experiment. Sudden decrease of temperature in fig. 2 indicates that water flooded the measuring point and high temperature indicates that steam is located at the measuring point. In numerical simulations no bubble entrapment is observed at measuring point T1. At the measuring point T2 the final temperature in simulations is lower then in the experiment. At the measuring point T3 and T4 the final local temperature in simulation is higher then in the experiment. When the water floods the measuring point T3 slow decrease of temperature is observed, which is even slower in simulations at finer meshes. In the experiment water flooding of the temperature measuring point is observed as sharp temperature decrease.

Integral condensation rate versus time in simulations calculated on different meshes is plotted on fig. 3. Large peak of condensation rate is at nearly the same time on all meshes (2.25±0.5 s) and appears at the same time as bubble entrapment is observed. During bubble entrapment the interfacial area and the turbulence kinetic energy is increased that is why also condensation heat transfer coefficient and condensation rate is increased. The value of the condensation rate peak remains nearly the same (0.39±0.02 kg/s) on all meshes. The mass of overall condensed steam is nearly the same on all meshes (0.4±0,014 kg).

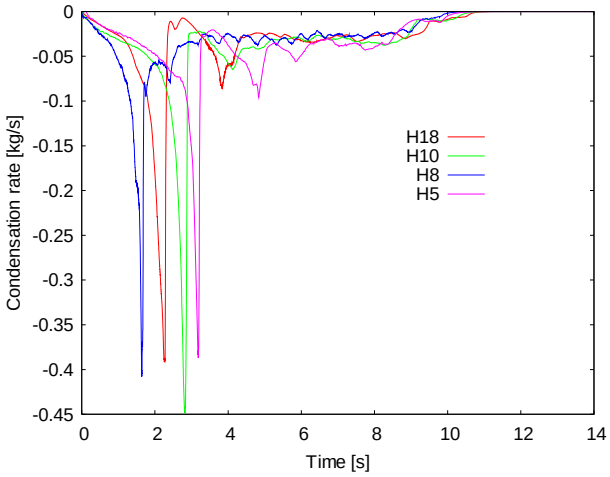

Figure 3**:** Condensation rate (integral) in simplified numerical simulations calculated on different meshes.

3.2 Numerical simulation of whole domain

We also performed numerical simulation of the whole domain. The inlet diameter is relatively small, that is why injected water forms a jet. Due to large inlet velocity of water the timestep must be very small, what increases CPU time. In the lower horizontal part two bubble entrapments are observed and in the upper horizontal part one smaller bubble entrapment is observed. The final local temperature in the numerical simulation (fig. 4) at the measuring point T2 is lower than in experiment and at measuring point T3 and T4 is higher than in experiment, what is also observed in simplified simulation. When the water floods the measuring point T3 slow decrease of temperature is observed, which is even slower in simulations on finer meshes. The mass of condensed steam is 0,463±0,036 kg, what is only slightly more then in the simplified simulation.

On fig. 5 the integral condensation rate is plotted versus time. Three peaks are observed at times which corresponds to three steam bubble entrapments. In the first period two bubble entrapments in lower horizontal part are observed; then filling of the vertical pipe follows; afterwards bubble entrapment in the upper horizontal pipe; then condensation on water

surface that is filling the horizontal pipe until pipe is completely filled with water. The condensation rate peak in upper horizontal pipe is much smaller in simulation of the whole domain then in the simplified simulation. This is due to the fact that water is preheated in the lower horizontal part and much less intense condensation occurs due to the smaller temperature difference.

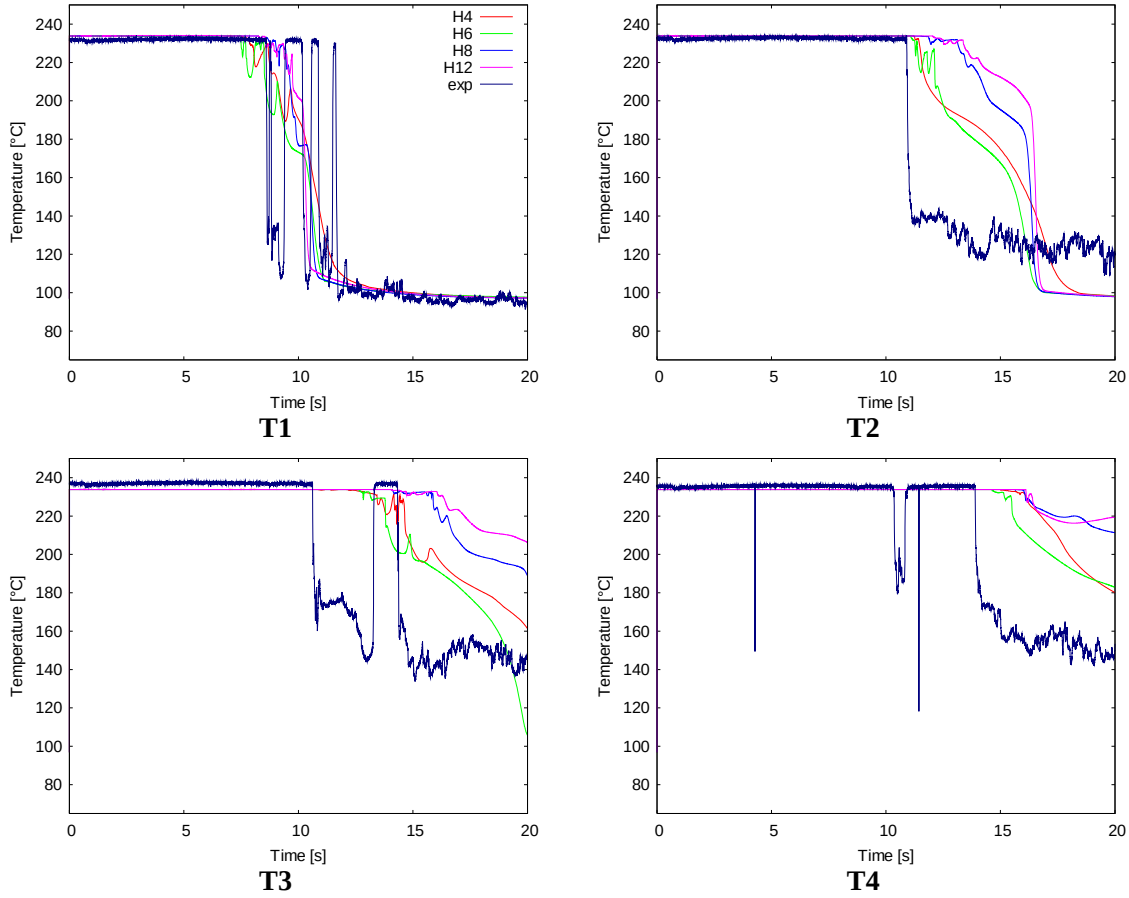

Figure 4**:** Local temperatures in numerical simulations of whole domain on different meshes and experiment at 4 measurement points.

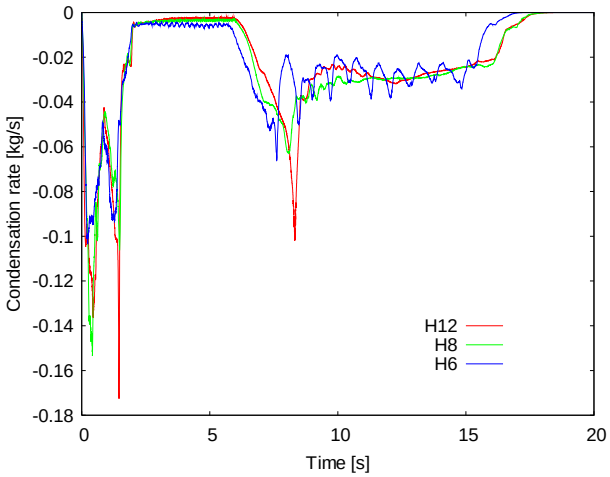

Figure 5**:** Condensation rate in numerical simulations of whole domain calculated on different meshes.

Volume fraction field at different time steps is plotted on fig. 6. The water jet can be observed at beginning (0.25 s). The state before the first two bubble entrapments is visible (0.25 s, 1 s) and the state before bubble entrapment in upper horizontal pipe (8 s) can also be seen. Filling of the upper horizontal pipe is visible at later times.

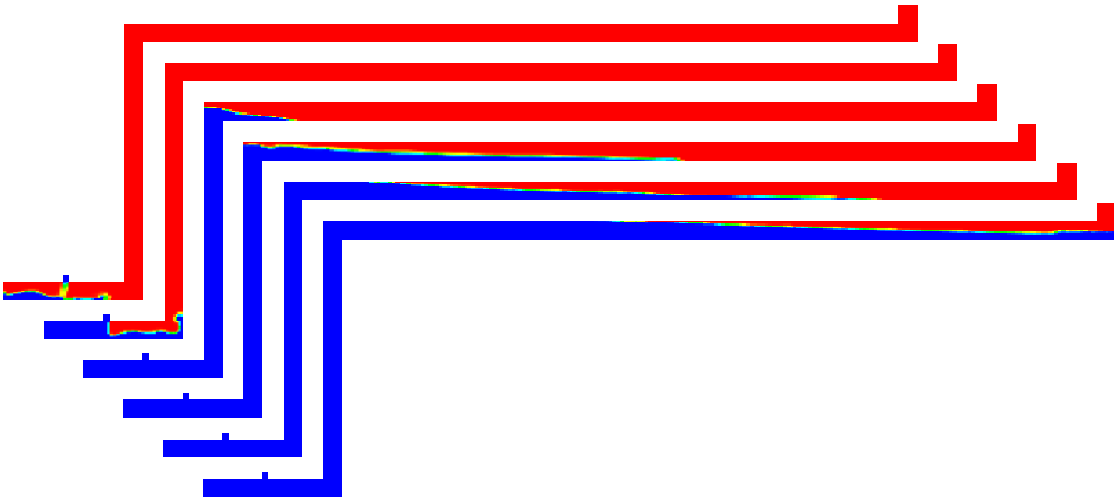

Figure 6**:** Volume fraction in simulation of whole domain at different time steps (0.25 s, 1 s, 6s, 8 s, 10 s, 14 s).

4 CONCLUSIONS

The ongoing work of CFD simulation of KFKI experiment is shown in this paper. The local temperature is not in good agreement with experiments due to stochastic nature of phenomena. We showed that during the bubble entrapment, the condensation rate is significantly increased. The evolution of local temperature is mesh dependent, but the overall mass of condensed steam is not mesh dependent. The water heat up is overestimated on all measuring points. In case where the whole domain was simulated the condensation rate during bubble entrapment in upper horizontal pipe was smaller then in simplified simulation, due to smaller temperature difference (preheated water in lower horizontal part). The simulation of KFKI experiment is a difficult task due to the fact that several bubble entrapments are present in upper and lower horizontal pipe. All bubble entrapments affects the condensation rate and increases the water temperature, which is the only parameter measured in experiment, which can be compared with simulation to verify the condensation model. The Hughes-Duffey correlation for direct contact condensation will be used in the further analysis with some modification which will decrease the condensation rate.

ACKNOWLEDGMENTS

The work was financially supported by the Slovene Ministry of Education, Science and Sport through the young researcher project 3311-04-831075 and NURESIM project in the framework of the Sixth Framework Program (2004-2007).

REFERENCES

[1] I. S. Lim, R. S. Tankin, M. C. Yuen, “Condensation measurement of horizontal cocurrent steam-water flow”, *Journal of Heat Transfer - T ASME*, 1984, **106**, pp. 425-432.

[2] H. J. Kim, S. C. Lee, S. G. Bankoff, "Heat transfer and interfacial drag in countercurrent steam-water stratified flow", *International Journal of Multiphase Flow*, 1985, **11**, pp. 593-606.

[3] W. Yao, P. Coste, D. Bestion, M. Boucker, "Two-phase pressurized thermal shock investigations using a 3D two-fluid modelling of stratified flow with condensation", *The 10th international Topical Meeting on Nuclear Reactor Thermal Hydraulics (NURETH-10)*, Seul, Korea, Oct. 5-9, 2003.

[4] C. Lorencez, M. Nasr-Esfahany, M. Kawaji, "Turbulence structure and prediction of interfacial heat and mass transfer in wavy-stratified flow", *AIChE Journal* , 1997, **43**, pp. 1426-1435.

[5] J. Mikielewicz, M. Trela, E. Ihnatowicz, "A theoretical and experimental investigation of dorect contact condensation on a liquid layer", *Experimental Thermal and fluid Science,* 1997, **15**, pp. 221-227.

[6] E. D. Hughes, R. B. Duffey, "Direct contact condensation and momentum-transfer in turbulent separated flows", *International Journal of Multiphase flow,* 1991, **17**, pp. 599-619.

[7] P. Coste, "Computational simulation of multi-D liquid –vapour thermal shock with condensation", *5th International Conference on Multiphase Flow (ICMF'04)*, Yokohama, Japan, May 30 – June 4, 2004, paper no. 420.

[8] M. Boucker, J. Lavieville, A. Martin, C. Bechaud, D. Bestion, P. Coste, "Preliminary applications of the new neptune two-phase CFD solver to pressurized thermal shock investigations", Proceedings of ICONE12 12th Conference on Nuclear Engineering, Arlington, Virginia, USA, April 25-29, 2004.

[9] J. Lavieville, E. Quemerais, M. Boucker, L. Maas, "NEPTUNE CFD V1.0 User Guide", 2005.

[10] H. M. Prasser, G. Ezsol, G. Baranyai, "PMK-2 water hammer tests, condensation caused by cold water injection into main steam-line of VVER-440-type PWR - Quick-Look Report (QLR)", *WAHALoads project deliverable D48,* 2004.

[11] H. M. Prasser, G. Ezsol, G. Baranyai, "PMK-2 water hammer tests, condensation caused by cold water injection into main steam-line of VVER-440-type PWR - Data Evaluation Report (DER)", *WAHALoads project deliverable D51,* 2004.

[12] Tiselj I., G. Černe, A. Horvat, J. Gale, I. Parzer, M. Giot, J. M. Seynhaeve, B. Kucienska, H. Lemonnier, "WAHA3 code manual", *WAHALoads project deliverable D10*, http://www2.ijs.si/~r4www/WAHA3_manual.pdf, 2004.

[13] J. Gale, I. Tiselj, "Water Hammer in horizontal water-steam counter-current flow", *proc. PVP2006-ICPVT-11, 2006 ASME Pressure Vessels and piping division conference*, 2006.

[14] J. Gale, I. Tiselj, I. Parzer, "Modelling of condensation induced water hammer", *Proc. of the 3rd International Symposium on Two-Phase Flow Modelling and Experimentation*, Pisa, Italy, September 22-24, 2004.